ELSEVIER

Available online at www.sciencedirect.com

ScienceDirect

Nuclear Physics A 00 (2020) 1–4

Nuclear Physics A

www.elsevier.com/locate/procedia

XXVIIIth International Conference on Ultrarelativistic Nucleus-Nucleus Collisions (Quark Matter 2019)

Measurement of global spin alignment of K^{*0} and ϕ vector mesons using the STAR detector at RHIC

Subhash Singha (for the STAR Collaboration)

Institute of Modern Physics Chinese Academy of Sciences, Lanzhou, Gansu, China 73000

subhash@impcas.ac.cn

Abstract

We report the transverse momentum (p_{T}) and centrality dependence of global spin alignment (ρ_{00}) of K^{*0} vector meson at midrapidity ($|y| < 0.5$) in Au + Au collisions at $\sqrt{s_{NN}}$ = 54.4 and 200 GeV with the STAR experiment at RHIC. The K^{*0} results are compared to that of ϕ meson. At low-p_{T} region and midcentral collisions, the K^{*0} ρ_{00} is found to be smaller than 1/3 with about 4σ significance, while that of ϕ meson is observed to be larger than 1/3 with about 3σ significance. The ρ_{00} results are compared between RHIC and LHC energies. The physics implication of our results is also discussed.

Keywords: relativistic heavy-ion collisions, vector meson, spin alignment

1. Introduction

In non-central heavy-ion collisions, a large initial global angular momentum ($\sim 10^4\hbar$) is expected [1]. This can induce a non-vanishing polarization for hadrons with non-zero spin via spin-orbit coupling. The measurement of spin polarization can offer new insight into the initial conditions and dynamics of the Quark-Gluon Plasma (QGP) [2, 3]. The STAR Collaboration reported significant non-zero Λ polarization at RHIC energies [4, 5]. This provides the first experimental evidence of the vorticity of the QGP medium induced by the initial angular momentum. The spin alignment of vector mesons can also be used to probe the vorticity [6]. The vector meson global spin alignment is quantified by the diagonal element of the spin density matrix (ρ_{00}) [7]. It is measured from the angular distribution of the decay daughter of the vector meson:

$$\frac{dN}{d\cos\theta^*} \propto \left[(1 - \rho_{00}) + (3\rho_{00} - 1)\cos^2\theta^*\right], \tag{1}$$

where θ^* is the angle between the polarization axis and momentum direction of the daughter particle in the rest frame of parent particle. For global spin alignment, the polarization axis is chosen as the direction perpendicular to the reaction plane which is correlated with the direction of the angular momentum of the colliding system. In the absence of spin alignment, the value of ρ_{00} is expected to be 1/3. Any deviation of ρ_{00} from 1/3 indicate a net spin alignment of vector mesons. Recent model calculations indicated that the ρ_{00} due to vorticity of the medium is expected to be smaller than 1/3, while that induced by the initial magnetic field can be larger or smaller than 1/3 depending on the electric charge of the vector meson [8]. It is also been predicted that different hadronization scenarios, such as the fragmentation and coalescence mechanisms can cause ρ_{00} to be larger and smaller than 1/3 [6]. The vector mesons, K^{*0} and ϕ, are expected to be produced predominantly from primordial production, unlike hyperons which are expected to have large resonance decay contribution. Another advantage is that the spin alignment of vector mesons are generally additive, whereas hyperons polarization are subject to local cancellation effects. Moreover, the lifetime of these vector mesons differ by a factor of ten, so they can carry informations of the medium from different time scale during its evolution.

2. Analysis method

This proceedings report the measurement of K^{*0} ρ_{00} at midrapidity ($|y| < 0.5$) in Au+Au collisions at $\sqrt{s_{\rm NN}}$ = 54.4 and 200 GeV. The minimum-bias events are selected by coincidence of east and west Vertex Position Detectors [9]. The charge particle tracking is performed using the Time Projection Chamber (TPC) [10]. The collision centrality is determined from the number of charged particles within $|\eta| < 0.5$ and corrected for triggering efficiency using a Monte Carlo Glauber simulation [11]. The 2^{nd}-order event plane (experimental approximate of reaction plane) is reconstructed using tracks inside the TPC. The particle identification is done using the specific ionization energy loss in TPC gas volume and the velocity of particles ($1/\beta$) measured by the Time-of-Flight (TOF) detector [12]. The K^{*0} ($\overline{K^{*0}}$) is reconstructed via hadronic decay channel: $K^{*0}(\overline{K^{*0}}) \rightarrow K^+\pi^-$ ($K^-\pi^+$) (branching ratio: 66%) [13]. Measurement of K^{*0} and $\overline{K^{*0}}$ are averaged and they are collectively referred to as K^{*0}. The combinatorial background is estimated from a pair rotation technique. The invariant mass signal is obtained after the subtraction of the combinatorial background. The signal is fitted with a Breit-Wigner distribution and a second-order polynomial function to take care of residual background. The yield is estimated by integrating signal histogram bins within the range: $(m_0 - 3\Gamma, m_0 + 3\Gamma)$, where m_0 and Γ are the invariant mass peak position and width of K^{*0}. The K^{*0} yield is obtained in five $\cos\theta^*$ bins, where the θ^* is the angle between the direction perpendicular to the 2^{nd}-order event plane and the momentum direction of daughter kaon in the rest frame of K^{*0}. The yield in each $\cos\theta^*$ bin is then corrected for detector acceptance and efficiency using a Monte Carlo embedding. We extract the observed ρ_{00} (denoted as $\rho_{00}^{\rm obs}$) by fitting the yield vs. $\cos\theta^*$ distribution using Eq. 1. The $\rho_{00}^{\rm obs}$ is then corrected for event plane resolution, following method detailed in [14], to obtain ρ_{00}:

$$\rho_{00} - \frac{1}{3} = \frac{4}{1+3R}(\rho_{00}^{obs} - \frac{1}{3}), \qquad (2)$$

where R is the TPC 2^{nd}-order event plane resolution, estimated from the correlation of two sub-events [15].

3. Results and discussions

3.1. Transverse momentum ($p_{\rm T}$) dependence

The solid star and circle markers in the left panel of Fig. 1 present the K^{*0} ρ_{00} measured using the 2^{nd}-order event plane as a function of $p_{\rm T}$ for 10-60% central Au+Au collisions at $\sqrt{s_{\rm NN}}$ = 54.4 and 200 GeV. The open markers present the ρ_{00} with respect to a three-dimensional (3D) random plane which is not expected to be correlated with the angular momentum direction. We observe that the ρ_{00} for $p_{\rm T} < 2.0$ GeV/c is smaller than 1/3 with about 4σ significance, while for higher $p_{\rm T}$ region the ρ_{00} is consistent with 1/3 within uncertainties. The ρ_{00} with respect to the 3D random plane is found to be consistent with 1/3 as expected. The observed deviation of K^{*0} ρ_{00} in low-$p_{\rm T}$ region can be qualitatively explained by models that consider the hadronization of polarized quarks via coalescence mechanism [6]. But to date, there is no quantitative estimate of K^{*0} ρ_{00} available from such models. The ρ_{00} of ϕ meson for $p_{\rm T}$=1.0–2.0 GeV/c in midcentral Au+Au collisions at $\sqrt{s_{\rm NN}}$ = 200 GeV (presented in QM2018) [16] is observed to be larger than 1/3. The ϕ ρ_{00} measurement does not fit into the naive quark coalescence or fragmentation model.

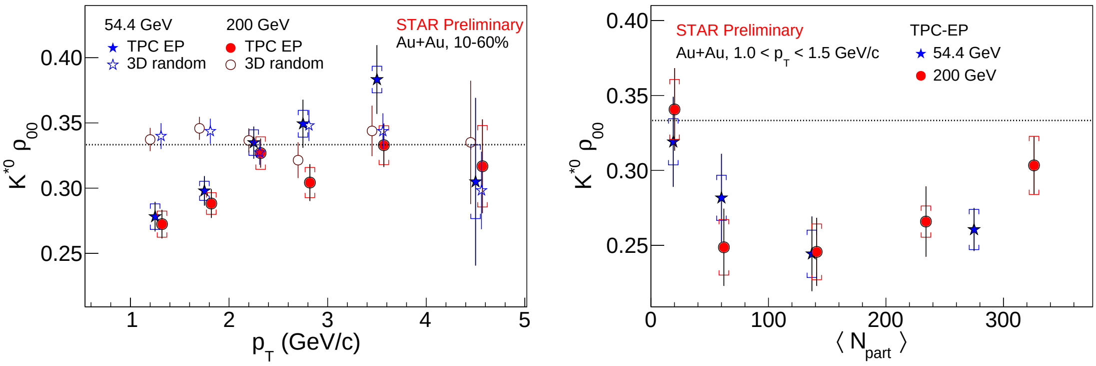

Fig. 1. Left panel: The solid circles and star markers present the K^{*0} ρ_{00} using the 2^{nd}-order event plane as function of $p_{\rm T}$ for 10-60% central Au+Au collisions at $\sqrt{s_{\rm NN}}$ = 54.4 and 200 GeV, respectively. The open markers present the same using a three-dimensional (3D) random plane. Right panel: The solid circles and star markers present the K^{*0} ρ_{00} using the 2^{nd}-order event plane as function of $\langle N_{\rm part}\rangle$ for $1.0 < p_{\rm T} < 1.5$ GeV/c. The vertical bars and caps denote statistical and systematic uncertainties, respectively.

3.2. Centrality ($\langle N_{\rm part}\rangle$) dependence

The right panel in Fig. 1 shows the K^{*0} ρ_{00} as function of average number of participating nucleons ($\langle N_{\rm part}\rangle$) for $1.0 < p_{\rm T} < 1.5$ GeV/c in Au+Au collisions at $\sqrt{s_{\rm NN}}$ = 54.4 and 200 GeV. We observed a clear centrality dependence with the maximum deviation of ρ_{00} from 1/3 in midcentral collisions. For peripheral collisions, the K^{*0} ρ_{00} is consistent with 1/3 while for most central collisions it is close to 1/3. The ρ_{00} of ϕ mesons (presented in QM2018) [16] shows similar centrality dependence, but with an opposite trend and the ρ_{00} is larger than 1/3 in midcentral collisions. Current models can not simultaneously explain the observed centrality dependence of ρ_{00} of K^{*0} and ϕ mesons.

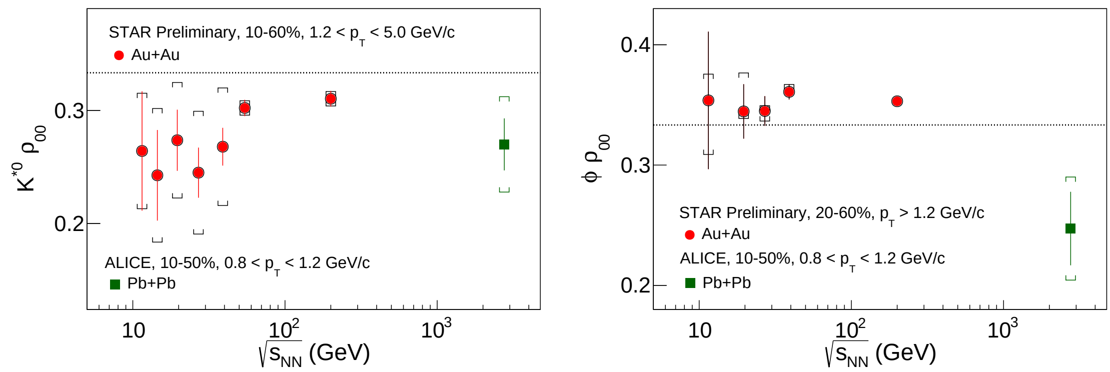

Fig. 2. Left panel: beam-energy dependence of K^{*0} ρ_{00} in midcentral collisions. Right panel: beam-energy dependence of ϕ ρ_{00} in midcentral collisions. In both panels, the vertical bars and caps denote statistical and systematic uncertainties, respectively.

3.3. Beam-energy ($\sqrt{s_{\rm NN}}$) dependence

The left panel in Fig. 2 presents the beam-energy dependence of K^{*0} ρ_{00} in midcentral collisions. The new measurements for Au+Au collisions at $\sqrt{s_{\rm NN}}$ = 54.4 and 200 GeV are compared to those from Au+Au collisions at $\sqrt{s_{\rm NN}}$ = 11.5 – 39 GeV reported in [16] and from Pb+Pb collisions at $\sqrt{s_{\rm NN}}$ = 2.76 TeV [17]. The K^{*0} ρ_{00} for low $p_{\rm T}$ and midcentral collisions is found to be smaller than 1/3 and within the present uncertainties no beam-energy dependence is observed. The right panel in Fig. 2 presents the beam energy dependence of ϕ ρ_{00}. The STAR results [16] from Au+Au collisions at $\sqrt{s_{\rm NN}}$ =11.5–200 GeV are compared to the measurements from LHC energies [17]. While the ϕ ρ_{00} in midcentral collisions at RHIC energies

Table 1. Sumary of ρ_{00} and P_H measurements at RHIC and LHC

Species	Quark content	J^P	ρ_{00}/P_H at top-RHIC	ρ_{00}/P_H at LHC
K^{*0}	$d\bar{s}$	1^-	$\rho_{00} < 1/3$ ($\sim 4\sigma$)	$\rho_{00} < 1/3$ ($\sim 3\sigma$)
ϕ	$s\bar{s}$	1^-	$\rho_{00} > 1/3$ ($\sim 3\sigma$)	$\rho_{00} < 1/3$ ($\sim 2\sigma$)
Λ	uds	$1/2^+$	$P_H > 0$; ($\sim 4\sigma$)	$P_H \sim 0$ ($\sim 1\sigma$)

is observed to be larger than 1/3 (about 3σ significance at 39 and 200 GeV), it is found to be smaller than 1/3 at the LHC energy (about 2σ significance). The trend of ϕ ρ_{00} at RHIC energies can be explained by a recent model calculation that considers the existence of coherent mesonic field [18]. Note that the calculation mentioned above does not exist for the K^{*0} meson.

4. Summary and conclusion

We presented p_{T} and centrality dependence of ρ_{00} of K^{*0} meson for Au+Au collisions at $\sqrt{s_{NN}}$= 54.4 and 200 GeV. At low p_{T} and midcentral collisions, the K^{*0} ρ_{00} is observed to be smaller than 1/3 with 4σ significance for both beam energies. This is an indication of K^{*0} spin alignment for both beam energies. For midcentral collisions, while the K^{*0} ρ_{00} is found to be smaller than 1/3, the ϕ ρ_{00} is observed to be larger than 1/3. It could be due to the different lifetime of these vector mesons and different responses to the vorticity of the medium at different time scales. No current theoretical model can explain simultaneously the trend of K^{*0} and ϕ ρ_{00}. Within the current precision, no significant beam-energy dependence is observed for K^{*0} ρ_{00}. The data from the 2^{nd} phase of the Beam Energy Scan in RHIC will improve the precision of the low energy data. The p_{T} and centrality dependence of ρ_{00} of K^{*0} is qualitatively similar between RHIC and LHC energies.

From the current theoretical understanding, the global hyperon polarization (P_H) is proportional to the quark polarization (P_q): $P_H \propto P_q$, while the spin alignment, $\rho_{00} \propto P_q^2$. Based on the above assumptions and the input of P_q from Λ polarization measurement, the expected ρ_{00} is close to 1/3. Hence, the current large deviation of ρ_{00} is surprising and poses challenges to theoretical understanding. Given the ρ_{00} can depend on multiple physics mechanisms, e.g. the vorticity, magnetic field, hadronization scenarios and mesonic fields, more theoretical efforts are required for understanding of the data.

References

[1] F. Becattini, F. Piccinini, J. Rizzo, Phys. Rev. **C77** (2008) 024906.
[2] Z.-T. Liang, X.-N. Wang, Phys. Rev. Lett. **94** (2005) 102301, [Erratum: Phys. Rev. Lett.96,039901(2006)].
[3] B. Betz, M. Gyulassy, G. Torrieri, Phys. Rev. **C76** (2007) 044901.
[4] L. Adamczyk, *et al.*, [STAR Collaboration], Nature **548** (2017) 6265
[5] J. Adam, *et al.*, [STAR Collaboration], Phys. Rev. **C98** (2018) 014910.
[6] Z.-T. Liang, X.-N. Wang, Phys. Lett. **B629** (2005) 2026.
[7] K. Schilling, P. Seyboth, G. E. Wolf, Nucl. Phys. **B15** (1970) 397412, [Erratum: Nucl. Phys.B18,332(1970)].
[8] Y.-G. Yang, R.-H. Fang, Q. Wang, X.-N. Wang **C97** (3) (2018) 034917
[9] W. J. Llope, *et al.*, [STAR Collaboration], Nucl. Instrum. Meth. **A522** (2004) 252273.
[10] M. Anderson, *et al.*, [STAR Collaboration], Nucl. Instrum. Meth. **A499** (2003) 659678.
[11] B. I. Abelev, *et al.*, [STAR Collaboration], Phys. Rev. **C79** (2009) 034909.
[12] B. Bonner *et al.*, Nucl. Instrum. Meth. **A508** (2003) 181184.
[13] M. Tanabashi, *et al.*,, Review of Particle Physics, Phys. Rev. **D98** (3) (2018) 030001.
[14] A. H. Tang, B. Tu, C. S. Zhou, Phys. Rev. **C98** (4) (2018) 044907
[15] A. M. Poskanzer, S. A. Voloshin, Phys. Rev. **C58** (1998) 16711678.
[16] C. Zhou, [for STAR Collaboration], Nucl. Phys. **A982** (2019) 559562.
[17] S. Acharya, *et al.*, [ALICE Collaboration], arXiv:1910.14408.
[18] X. Sheng, L. Oliva, Q. Wang, arXiv:1910.13684